Nanoscale

Accepted Manuscript

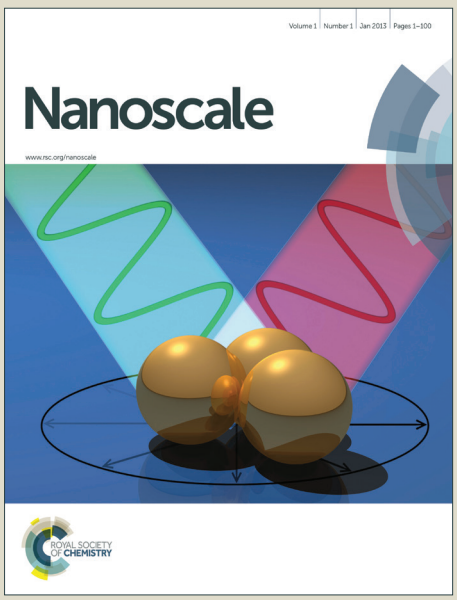

ROYAL SOCIETY OF CHEMISTRY

www.rsc.org/nanoscale

Journal Name

RSCPublishing

ARTICLE

On the Role of Localized Surface Plasmon Resonance in VU-Vis Light Irradiated Au/TiO_2 Photocatalysis System: Pros and Cons

Cite this: DOI: 10.1039/x0xx00000x

Received 00th January 2012,
Accepted 00th January 2012

DOI: 10.1039/x0xx00000x

www.rsc.org/

Zhongjin Lin,[a, c] Xiaohong Wang,[b, c] Jun Liu,[d, c] Zunyi Tian,[a, c] Loucheng Dai,[a, c] Beibei He,[b, c] Chao Han,[a, c] Yigui Wu,[a, c] Zhigang Zeng,[a, c] and Zhiyu Hu*[c, e]

The role of localized surface plasmon resonance (LSPR) in UV-Vis light irradiated Au/TiO_2 photocatalysis system has been investigated, and it is demonstrated experimentally for the first time that both pros and cons of LSPR exist simultaneously on the photocatalytic reaction. We have proved that when operating under mixing UV and green light irradiation, the LSPR injected hot electrons (from Au nanoparticles to TiO_2 under green light irradiation) may surmount the Schottky barrier (SB) forming between Au nanoparticles and TiO_2, and flow back into the TiO_2. As a result, these electrons may compensate and even surpass those transferred from TiO_2 to Au nanoparticles, thus accelerates the recombination of UV excited electron-hole pairs in TiO_2. This is the negative effect of LSPR. On the other hand, more hot electrons existing on the Au nanoparticles surface due to the LSPR would favor the photocatalytic reaction, which, accompanied by the negative effect, dominate the overall photocatalytic performance. The presented result reveals the multi-faceted essence of LSPR on Au/TiO_2 structure, and is instructive for the application of metal-semiconductor composite in the photocatalysis. Moreover, it is confirmed that what extent would the above pros and cons of LSPR respectively dominate the overall photocatalytic reaction depends on the intensity ratio of visible to UV light.

1. Introduction

Since the first discover by Fujishima and Honda et.al. in 1972 that titanium dioxide (TiO_2) electrode showed an outstanding photocatalytic activity towards water splitting reaction,[1] TiO_2 based materials have attracted growing interest in the fields of effective utilization of solar energy in environmental purification, organic synthesis, water splitting for hydrogen generation and so forth.[2-4] Unfortunately however, the TiO_2 has a relatively large band gap energy (anatase, E_g = 3.2 eV; rutile, E_g = 3.0 eV),[5] which limits the effective photonic excitation on the solar light range.[6] Constructing visible light TiO_2-based photocatalyst is therefore of significant importance. To date, much effort has been made to optimize the photocatalyitc performance such as band-gap engineering by doping,[7] building composite structure by combing graphene[8] or metal nanoparticles (NPs) decoration[9, 10]. Typically, localized surface plasmon resonance (LSPR), which arises from the collective oscillations of the conduction electrons induced by light irradiation, has been successfully applied to enhance the photocatalytic performance of TiO_2 for its promising capacity to achieve visible light response.[11, 12]

Previous works have demonstrated that, irradiating Au/TiO_2 with visible light, the electrons in Au NPs excited by the LSPR will transfer from Au NPs to the TiO_2, which facilitates reduction half-reaction.[9, 13] On the other hand, if Au/TiO_2 is exposed to ultraviolet (UV) light, the Au NPs will trap photogenerated electrons and play a role as electron donor.[1, 3, 14] More often than not, the application of photocatalysis is expected to operate under the natural condition, say, the sunlight irradiation with a wide range of wavelength from UV to visible. Therefore, the next question should come to which role would LSPR play in the photocatalytic reaction with Au/TiO_2 structure under ultraviolet-visible (UV-Vis) light irradiation. Typically, Yan and coworkers illustrated that the photocatalytic performance of Au/TiO_2 under UV-Vis light irradiation was significantly higher than that under UV light irradiation, merely emphasizing the positive effect of LSPR.[11] Is that the whole picture? Here, by investigating the photocatalytic behavior of Au/TiO_2 structure under UV-Vis mixing light irradiation, we will give a more comprehensive understanding about both sides of the coin that pros and cons of LSPR may exist simultaneously on the UV-Vis photocatalysis.

First of all, for better understanding of the mechanisms of plasmonic photocatalysis, it is crucial to reveal the essence of metal-semiconductor (M-S) interfaces. For Au/TiO_2 photocatalysis, Schottky barrier (SB) is one of the prominent features.[15] However, it has been reported that M-S nanocontact is quite different compared with their macroscopic counterpart.[16, 17] For example, Kraya and coworkers have demonstrated that the transportation of electrons between Au and $SrTiO_3$ had a transition from thermionic emission dominated to tunneling dominated, leading to ohmic behavior, as the interface sizes decrease continuously.[18] In our experiment, conductive atomic force microscopy (CAFM) was applied to characterize the SB contact feature at nano-Au/TiO_2 interfaces. The acquisition of current-voltage (*I-V*) curves allowed us to analyze the interface structure with thermionic emission (TE) theory.

Recently, Berger et al. have reported the process of photogenerated electrons been trapped at shallow trap of energy ~0.1 eV below the conduction band (CB) edge.[19, 20] The shallow trapped electrons excitation from a shallow trap to a continuum of states in the CB of TiO_2 may result in a broad IR absorption (called shallow trap IR absorption, STIRA).[20] In this paper, to probe the electrons transfer between Au NPs and TiO_2 due to LSPR, we have proposed a novel ATR-IR based method measuring the STIRA of Au/TiO_2 under the green light. Typically, the duration of electrons transfer process is so short (femto to milliseconds)[21] that is hard to observe, the electrons transfer from the Au NPs into TiO_2 however, can be trapped at shallow trap of TiO_2 for hours.[19] Therefore, the STIRA peak of Au/TiO_2 detected during green light excitation can be used to investigate the electron transfer behavior.

2. Experimental

2.1. Fabrication of TiO_2 Thin Films

Prior to use, indium-tin oxide glass (ITO, a size of $20\times20\times1.1$ mm^3 and sheet resistance of 6 Ohms sq^{-1}) pieces were rinsed with acetone, methanol, and deionized water in an ultrasonic bath for 10 min and then was immersed into isopropanol solution.[22] The TiO_2 thin films were fabricated according to the previously reports.[23, 24] Commercial type anatase TiO_2 colloid (Totitan New Materials Co.) was doctor-bladed onto the ITO glass substrate and air dried at the room temperature. After 30 minutes, the deposited films were placed into the annealing furnace and annealed with gradually increasing temperatures, i.e 125 °C (6 min), 325 °C (15 min), 375 °C (10 min), 450 °C (15 min), and 500 °C (10 min).

2.2. Fabrication of Au/TiO_2 Thin Films

The starting materials, $HAuCl_4\bullet3H_2O$, K_2CO_3, tannic acid and sodium citrate were purchased from Shanghai Chemical Reagents Corporation (SCRC). A solution of $HAuCl_4\bullet3H_2O$ (0.25 mL, 1 wt %) was dissolved in 20 mL of deionized water (Millipore) in a conical flask and heated to 60 °C. Under vigorous stirring, a mixed solution (8ml) of sodium citrate (4 wt %), K_2CO_3 (5 mM), tannic acid (1 wt %) and deionized water (quality ratio = 1: 0.05: 0.1: 18.85) was added. After the reaction, the mixture was maintained at 60 °C for 30 min and followed by deionized water (15 ml, 60 °C) injection. Then 3ml of above reaction mixture was shifted to a small glass beaker doctored with the prepared TiO_2 thin films. At the same time, we put the glass beaker into loft drier under 60 °C until the water was dried, so that Au NPs can be deposited on the surface of the TiO_2 thin films.

2.3. Characterization

The absorption spectra were recorded using UV-Vis spectrophotometer (UV- 2501PC). The theoretical light absorption cross section and the charge distribution were calculated by the finite element method (FEM) on the commercial simulation software (COMSOL Multiphysics 4.2). The morphology of the samples was investigated by using a field emission scanning electron microscopy (FESEM, Zeiss, ULTRA55). Particle size and shape were analyzed with image magnification. The high-resolution transmission electron microscopy (HRTEM) images were taken by a JEM-2010F high-resolution transmission electron microscope operating at 200 kV. The energy-dispersive X-ray spectroscopy (EDS, JEM-2010F) was carried out to confirm the composition of Au NPs and the dispersion information about Au NPs. X-ray diffraction (XRD) analysis was performed on a DLMAX-2200. Diffraction patterns were recorded with Cu Kα radiation (40 mA, 40 kV) over a 2θ-range of 10° to 70° and a position-sensitive detector using a step size of 0.06° and a step time of 1 s. The X-ray photoelectron spectroscopy (XPS) characterization was measured by using ESCALAD250XI (Al Kα radiation, h υ = 1486.6 eV) with a pass energy of 30 eV. The formation of Schottky nanocontacts of Au NPs on TiO_2 thin films substrates was measured with the CAFM model by an Atomic Force Microscope (AFM, Dimension Edge, Bruker). This method allows for the acquisition of *I-V* curves at known loading forces with minimal disruption to the interfaces during imaging.

2.4. STIRA Measurement

Infrared spectra were recorded using a Nicolet iS10 FT-IR equipped with a MCT Liquid Nitrogen detector. The resolution was 4 cm^{-1} and spectra were averaged over 64 scans. Irradiation of samples with light as shown in Figure S1 was carried out using a 365-nm small power of UV light-emitting diode (SUV-LED, power of 1W) and the 525-nm small power of green light-emitting diode (SG-LED, power can be adjusted from 1W to zero). A DuraSampl IR 3-mm diameter diamond-faced 1 reflection ZnSe prism (ASI SensIR Technolo-gies) was used in the ATR-IR measurements. Room temperature was regulated at 23 ± 1 °C. The air humidity was kept at 45 ± 2%. (Scheme of the ATR-FTIR cell, including the SUV-LED and SG-LED, was shown in Figure S1, Supporting Information)

2.5. Photocatalytic Activities Measurement

We prepared 10 mg/L methylene blue (MB) solution as the reactant to test the photocatalytic activity of the samples. The samples immersed in 6 ml of MB solution was irradiated by the

mixing light of the 365-nm high power of UV light-emitting diode (HUV-LED, power of 10 W, ~10 nm fwhm) and the 525-nm high power of green light-emitting diode (HG-LED, power can be adjusted from 20 W to zero, ~10 nm fwhm). The suspension was under the dark for 20 min to attain the adsorption equilibrium of the MB molecules on the photocatalyst surface and continuously purged with air to ensure a constant O_2 concentration throughout the experiment. The concentration change of MB was measured by UV-Vis spectrometry (UV-2501PC) following its 664 nm characteristic band.[10]

3. Results and discussion

3.1. Characterization

The TiO_2 in our experiments is entirely anatase phase (as shown in Figure S2). Two weak Au diffraction peak were observed at 2θ = 38.18° (111), 64.15° (220).[25] Such weak Au diffraction peak may result from the low metal content or crystalline domain of the metal NPs deposited.[26] To study the valence states of the Au, the Au/TiO_2 was analyzed with XPS by the Au 4f peak, and the corresponding results are shown in Fig. 1a. The main Au 4f 7/2 component is located at a binding energy of 83.12 eV which can be assigned to the Au in the zero-valent state.[27] No shoulder peak can be observed at higher binding energies (Au^+ 4f 7/2 at 84.5 eV and Au^{3+} 4f 7/2 at 85.6 eV) in the spectra,[10] indicating that the gold is present only in its metallic form.

Typical SEM micrograph of the Au/TiO_2 is shown in Figure 1b. The Au NPs are distinguishable in the micrograph, revealing that the Au NPs were successfully and uniformly deposited on the surface of TiO_2. This can be attributed to the overdose of sodium citrate as stabilizing agent avoiding the reunion of Au NPs during the process of deposition.[28] Particle diameters were analyzed with image magnification, and the statistical mean diameter of Au NPs is 10.42 nm. Figure 1c displays the EDS linescan profile recorded on Au/TiO_2, which confirms that the big and small particles are TiO_2 and Au, respectively. In Figure 1e, the HRTEM image taken at the interface of Au NPs and TiO_2 region clearly reveals two distinct sets of lattice fringes, which can be, respectively, assigned to anatase TiO_2 and face-centered cubic Au. The Au/Ti weight percentage of our Au/TiO_2 samples was 2.16% in accordance with the EDS analysis (Figure S3).

3.2. Optical Absorption

The light absorption behavior of the studied Au/TiO_2 is shown in Figure 2a. The strong absorption observed at around λ = 350 nm corresponds to the band-band transition of bare TiO_2.[1] By comparing the absorption spectra of bare TiO_2, a typical absorption peak can be observed at around λ_{max} = 536 nm on Au/TiO_2, which can be attributed to the LSPR of Au NPs.[11, 29] Specially, this absorption peak, appearing in visible light region, is responsible for Au/TiO_2 visible light response as will be shown later on. Besides, the surface plasmon absorption of Au NPs deposited on TiO_2 surface has a red shift comparing with that of Au NPs immersed into water.[3, 15] The different dielectric constant of environment surrounding the Au NPs causes the red shift.[3, 30, 31] The red shift is in good agreement with FEM simulations, which are displayed in Figure 2b (see Supporting Information for details). It is noteworthy that the red shift of the computational result is larger than the experimental result, which may be contributed to the inhomogeneous shape and size of the Au/TiO_2 nanostructures.

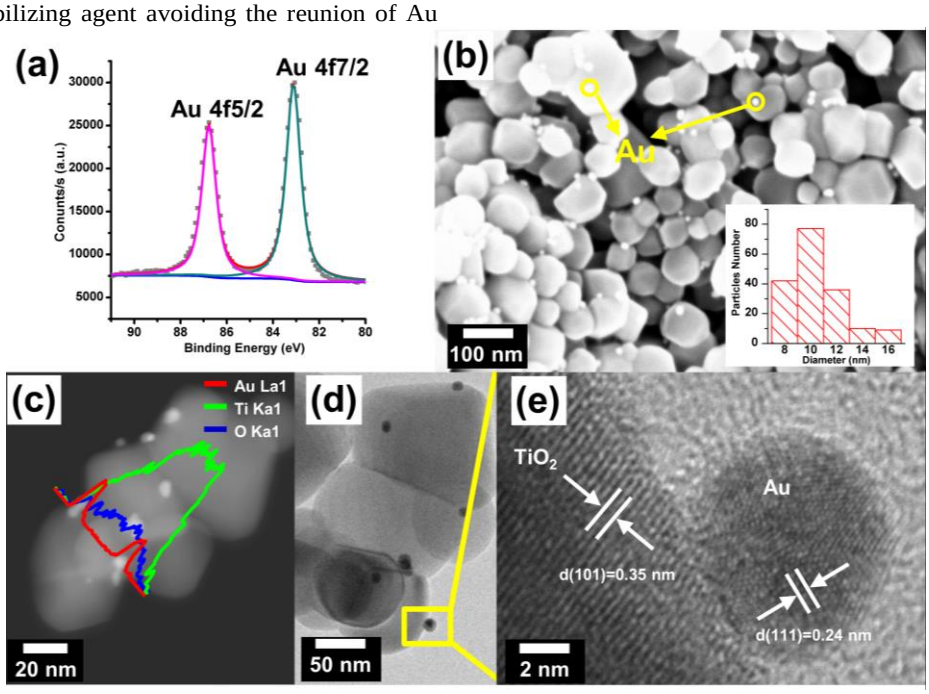

Figure 1. (a) XPS spectra of Au/TiO_2, (b) SEM image of Au/TiO_2, inset: size distributions of Au NPs, (c) EDS linescan profile of Au/TiO_2, (d, e) HRTEM image taken at the interface between Au NR and TiO_2.

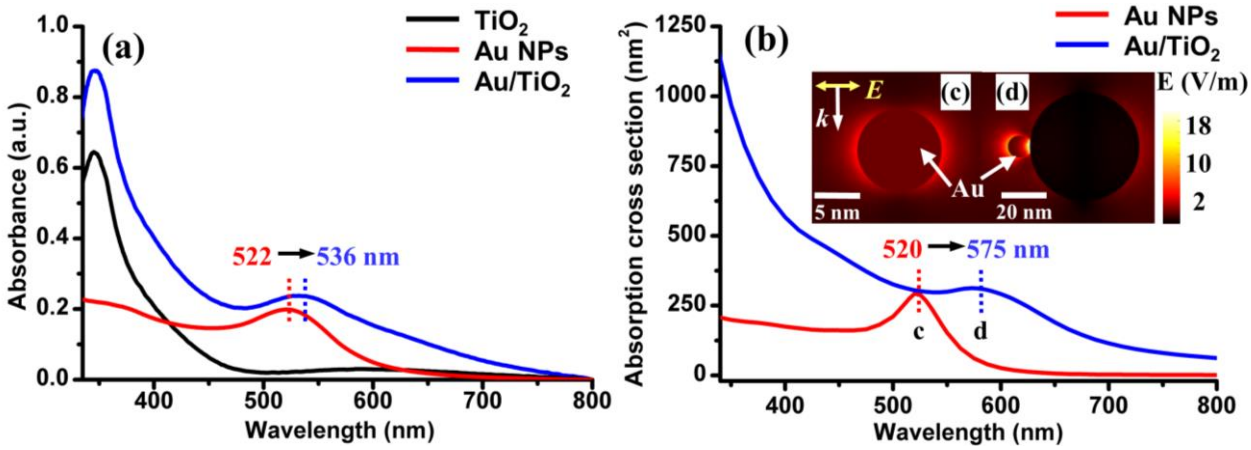

Figure 2. (a) Experimental UV-Vis absorption spectra of bare TiO_2 (black line), Au NPs (red line) and Au/TiO_2 (blue line). (b) Simulated absorption cross section spectrum of Au NPs (red line), Au/TiO_2 (blue line). Simulated electric field intensity patterns for (c) Au NPs (10 nm) at a wavelength of 520 nm and (d) Au/TiO_2 at a wavelength of 575 nm.

3.3. Photocatalytic Activity of Au/TiO_2

To ensure the selective excitation of LSPR on the Au NPs, the green light with 525 nm central wavelength was selected as visible light source for the photocatalytic activity measurement. Photocatalytic activity of the Au/TiO_2 samples, under different light irradiation, was evaluated following the reaction of MB. The activities of all different light irradiated samples were estimated by taking the initial 4 hours of MB disappearance (mg/L), represented in Figure 3. In this article, X W green light and Y W UV light irradiated Au/TiO_2 will be denoted as X/YW/Au/TiO_2. For example, 12/10W/Au/TiO_2 means the Au/TiO_2 is excited by the mixing light of 12 W green light and 10 W UV light. Firstly, when merely applied with green light irradiation, the 20/0W/Au/TiO_2 shows some photocatalytic activity despite that the photon energy of green light source is less than the band gap energy of TiO_2. Obviously, this can be ascribed to the effect of photo-excited plasmonic Au NPs. Detailed discussion about the photoexcited charge transfer in the Au/TiO_2 exposure to the visible light will be shown later on. In addition, the pure Au NPs irradiated by green light do not exhibit photocatalytic activity, so that the photocatalytic reaction induced by pure Au NPs under green light irradiation can be neglected in our experiment. As shown in Figure 3, during the irradiation of UV light, the photocatalytic activity of Au/TiO_2 is higher than that of pure TiO_2, because the Au NPs can trap photogenerated electrons and then inhibit the recombination of photogenerated electron-hole pairs. Next, it is interesting that the synergetic excitation of UV and visible light can promote the photocatalytic activity of Au/TiO_2. Moreover, it can be found that the activity of the Au/TiO_2 is not linear with green light intensity. With increasing power ratios of green to UV light, the photocatalytic activity of Au/TiO_2 enhances firstly and then rapidly changes into decline, but increases again at last. Assuming that the LSPR of Au NPs only has positive effect, the photocatalytic activity would rise continuously with increasing visible light intensity, which contradicts our experimental observation as discussed above. Another question is that, the photocatalysis arising from LSPR is very weak under the single visible light irradiation, but when adding the UV light, the LSPR exhibit a distinct influence on the photocatalysis. Accordingly, we propose a dual-effect mechanism of LSPR on the UV-Vis photocatalytic reaction, of which the details will be demonstrated in this paper.

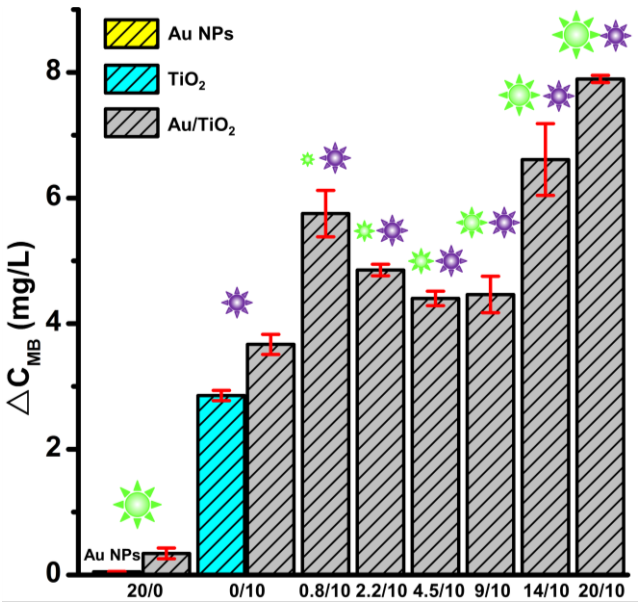

Figure 3. The activity of Au NPs, TiO_2 and Au/TiO_2 under different power ratios of green to UV light irradiation.

3.4. The Nanocontacts Characterization of Au/TiO_2

Compared with the single semiconductor photocatalysis, the photocatalysis of metal NPs and semiconductor nanocomposites possesses two distinct features, SB and LSPR.[15, 32] The SB can prevent low energy electrons from shuttling freely between the metal and semiconductor, so that suppresses the recombination of photogenerated electron-hole pairs.[33] The existence of SB is one of the most important factors for obtaining drastic enhancement of photoreactivity as dispersing metal NPs on semiconductor photocatalysts.[34] Despite of the large volume of

previous reports on LSPR photocatalysis,[26, 35-37] few work has shed light on the characterization of Schottky nanocontacts on these M-S structure photocatalyst, thus remaining a shadow on their contact quality. Here, this article will reveal more detailed information about the SB of Au/TiO_2 via the *I-V* characterization. (The contact between CAFM tip and bare TiO_2 is ohmic, and the *I-V* characterization of them has been discussed in Supporting Information.)

The *I-V* curves of Au/TiO_2 nanocontacts of different positions (A, B, C, D, E) on the thin film are shown in Figure 4a. It is obvious that the I-V curves vary from different positions detected by CAFM, which possibly originates from the different nanocontact area between Au NPs and TiO_2 (Figure 4b-f). According to TE theory, the current across Schottky contact is given by[16, 17, 38]

$$I = I_0 \exp\left(\frac{-qU}{nkT}\right)\left[1-\exp\left(\frac{qU}{kT}\right)\right], \quad (1)$$

where I_0 is the saturation current, n is the ideality factor, which be defined by

$$I_0 = SA^*T^2 \exp\left(\frac{-q\Phi_{b0}}{kT}\right), \quad (2)$$

$$n = \frac{q}{kT}\left(\frac{dU}{d(\ln I)}\right), \quad (3)$$

where U is the applied bias voltage, k is Boltzmann constant, T is the temperature in Kelvin, q is the charge of the electron, S is the contact area, A^* is the effective Richardson constant and equals to 24 $A\cdot cm^{-2}\cdot K^{-2}$ for anatase TiO_2,[32] Φ_{b0} is the Schottky barrier high (SBH).

By fitting the linear portion of the negative biased *I-V* curves of the real Schottky contacts to the relation derived for equation 1, 2 and 3, the saturation current I_0, SBH Φ_{b0} and ideality factor *n*, could been calculated shown in Table 1 (see Supporting Information for details).[38, 39] If we regarded a half of surface areas of Au NPs as the contact area, the approximate average Φ_{b0} = 0.36 eV was acquired. Obviously, the average SBH of our Au/TiO_2 samples is much less than the SBH of larger macroscopic contacts of Au and TiO_2 (Φ_{b0} = 1.2 eV).[40, 41] According to the report of Govorov et al, the differences of size, orientation, and structure at the interface could made this discrepancy.[42] All the value of n calculated is higher than 2 indicating that the ratio of tunneling to thermionic emission at Au/TiO_2 interface is of high level, which means the charge transport across the interface only is no longer due to thermionic emission.[43] But the high ideality factors may also be caused by a part of CAFM tip direct contact with TiO_2. However, we have demonstrated that the nanocontacts of Au NPs and TiO_2 with the interface diameter of less than 10nm are not the ohmic contacts but the Schottky contacts in our research. Therefore we can elucidate our experiment base on SB, especially when the experiment relates to the electrons transfer between the Au NPs and TiO_2.

Table 1. The value of various parameters determined from I-V characteristics of Au/TiO_2 at 300 K. (S_A,S_B···S_E (100 nm^2) are the corresponding contact area)

Line	I_0 (10^{-3} nA)	Φ_{b0} (eV)	n
A	2.60176	0.35+ln(S_A)/38	2.2097
B	2.86276	0.34+ln(S_B)/38	2.3785
C	0.40038	0.40+ln(S_C)/38	2.4136
D	9.18715	0.32+ln(S_D)/38	3.8752
E	17.89406	0.30+ln(S_E)/38	3.9205

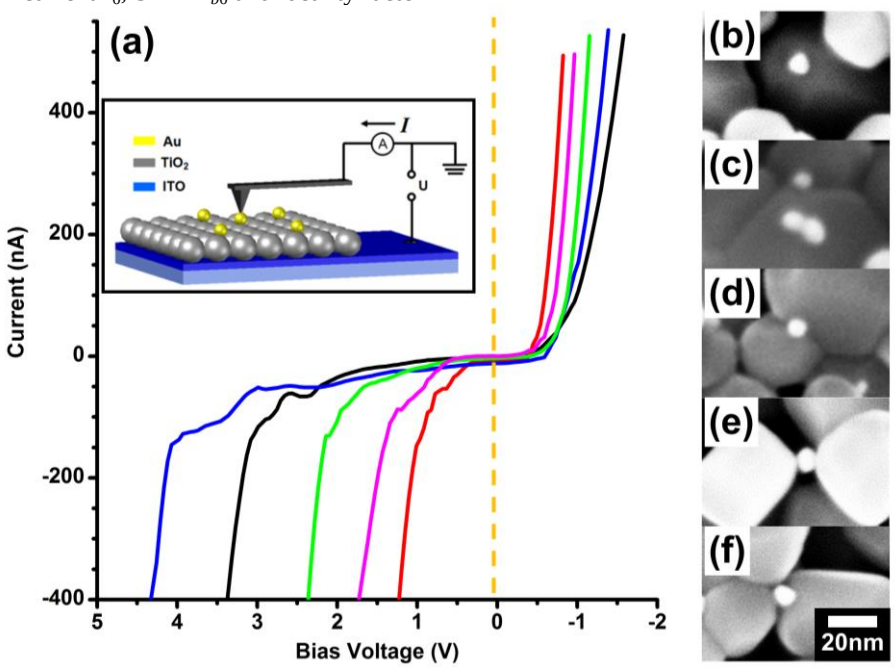

Figure 4. (a) Typical I-V curves for the Au/TiO_2 interfaces of different positions (A, B, C, D, E) of thin films. The inset shows the schematic representation of the CAFM (forward current in accordance with direction arrow), (b, c, d, e, f) SEM images of different contact modes between Au NPs and TiO_2 (white dots are the Au NPs).

3.5. Estimation of Photoexcited Charge Transfer between Au NPs and TiO_2 due to the LSPR

The works of previous people have demonstrated that, the stabilization of electrons localized on shallow trap of TiO_2 can be stored for hours,[21] and it can be easily measured by IR absorption spectra. In this paper, the shallow trap of TiO_2 will be applied to observe the photoexcited charge transfer between Au NPs and TiO_2 when irradiated with green light.

The electron and hole pairs are produced in TiO_2 under UV irradiation. And then the photogenerated electrons migrate to shallow traps and tend to reduce Ti^{4+} cations to Ti^{3+} states.[44] The charge transfer steps are as follows,[45]

$$TiO_2 + h\nu \rightarrow e^-_{CB} + h^+_{VB} \quad (4)$$

$$e^-_{CB} + Ti^{4+} \rightarrow Ti^{3+} \text{ trapped electron} \quad (5)$$

The excitation of trapped electrons can result in a STIRA. As shown in Fig. 5a, the TiO_2 can produce a prominent IR absorption during UV irradiation. If the photons with energy less than the band gap of TiO_2 are absorbed, the STIRA would not appear, such as the green light applied to irradiate TiO_2 is unable to excite IR absorption (Figure 5a). While by using the same green light to irradiate Au/TiO_2, an obvious IR absorption peak at ~850 cm^{-1} can be observed (show in Figure 5b).[21] In addition, the sample of Au/TiO_2 under UV light irradiation also appears an IR absorption peak at ~850 cm^{-1} (show in Figure 5b), which can be ascribed to the STIRA (the scenario is illustrated in Figure 5c). By comparing Figure 5a and b, we can conclude that the IR absorption of Au/TiO_2 under the green light is the result of STIRA. Due to the fact that green light irradiation of TiO_2 could not create electron-hole pairs, the electrons trapped at shallow trap should not come from the valence band of TiO_2, but from the Au NPs. Therefore, the possible electron generation-transportation mechanism could be: (1) LSPR excitation in Au NPs under green light irradiation, meanwhile, the hot electrons production from the LSPR decay,[46] (2) hot electrons injection from Au NPs to TiO_2 overleap SB (we have proved the existence of SB between Au NPs and TiO_2 in above section), (3) hot electrons reside in the shallow trap forming Ti^{3+} centers. [47, 48] The above processes can be concluded as the following formulas, which are also depicted in Figure 5d:

$$\text{Au NPs} + h\nu \rightarrow \text{Hot electrons} \quad (6)$$

$$\text{Hot electrons} \xrightarrow{\text{Overleap SB}} e^-_{CB} \quad (7)$$

$$e^-_{CB} + Ti^{4+} \rightarrow Ti^{3+} \text{ trapped electrons} \quad (8)$$

These are the direct proofs of which the photoexcited electrons in the Au NPs have sufficient energy to overleap the SB and flow into the CB of TiO_2. Although the conventional IR spectroscopic observation of trapped electrons have been studied for ages,[44] the way using the STIRA to prove this process is novel. And even it suited to all the composite structures of metal NPs and TiO_2.

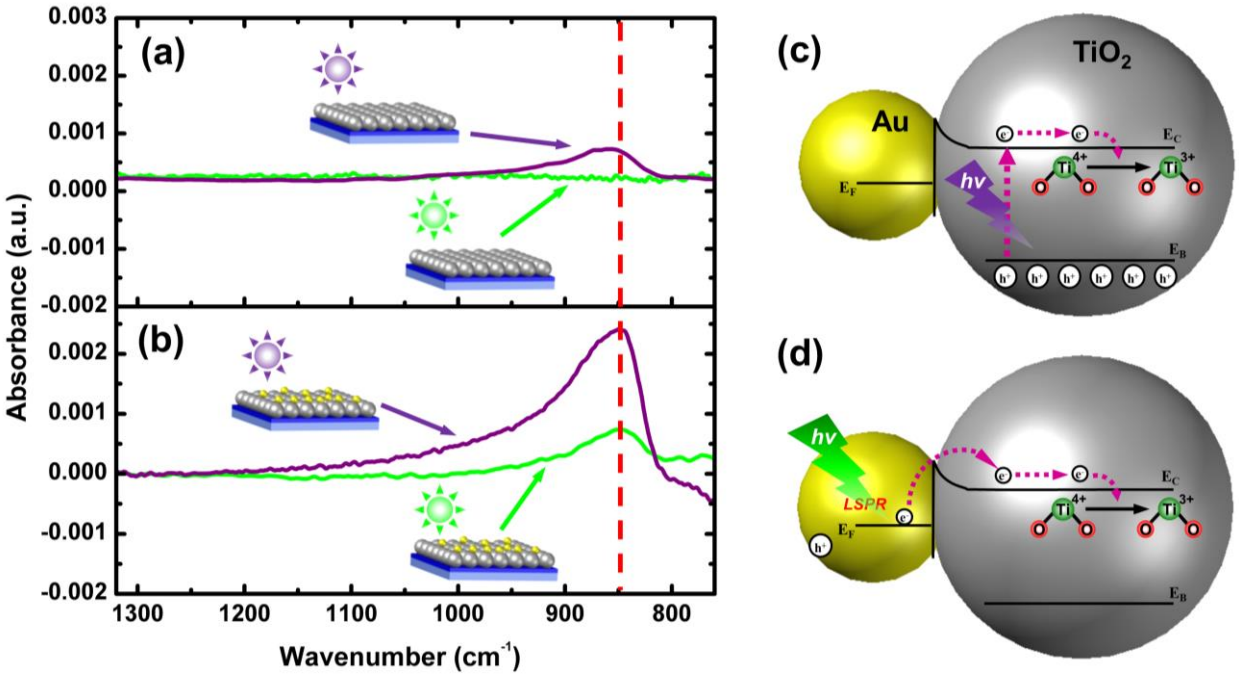

Figure 5. ATR-IR spectrum of (a) bare TiO_2 nanoparticle films under the green light (green line) or VU light (amethyst line) irradiation, (b) Au/TiO_2 under the green light (green line) or VU light (amethyst line) irradiation. All of background spectrums are before the light irradiation. The charge transfer steps in the Au/TiO_2 (c) under the UV light irradiation, (d) under the green light irradiation.

3.6. The Effect Mechanisms of LSPR on the Photocatalysis

STIRA is a convenient probe for observing the kinetic behaviors of the electrons recombined with the complementary holes.[49-51] The STIRA maximum intensity is corresponding to the concentration of photogenerated electrons in TiO_2.[21, 52] If a successive UV light is irradiated on TiO_2, the photogenerated electrons will be accumulated in TiO_2, and their concentration will increase until reaching the equilibrium sate, when the rate of electron generation and recombination is identical.[53, 54] Un-

der a given UV light irradiation, the maximum concentration of photogenerated electrons in TiO_2 is proportional to the lifetime of photogenerated electrons,[54, 55] and is given by the equation as follow,

$$[e] = \alpha\beta I\tau_e \quad (9)$$

where [e] is the concentration of photogenerated electrons at steady-state conditions, α is the absorption coefficient of TiO_2, β is the quantum yield, I is the incident light intensity and τ_e is the lifetime of photogenerated electrons. Therefore, both the concentration and the lifetime of photogenerated electrons can be determined by the STIRA maximum. Here, we defined the STIRA maximum which corresponds to the steady-state concentration of photogenerated electrons, as steady-state STIRA maximum (SSIRMax). In order to investigate the influences of LSPR on the lifetime of photogenerated electrons under UV-Vis light irradiation, the in-situ ATR-IR spectrum of different light-irradiated Au/TiO_2 was recorded and the data is presented in Figure 6. It is evident that the SSIRMax merely under UV light irradiation is higher than that induced by UV-Vis light. In addition, the intensity of UV light remains constant, the SSIRMax continues to decrease with the gradual increase of the green light power (Figure 6b), but the trend become weaker. This reveals that, to a certain extent, the LSPR of Au NPs created in response to the visible light, may reduce the lifetime of electrons which are produced from TiO_2 valence band by UV light excitation. This suggests that, the negative effect of LSPR derives from shortening the lifetime of electrons.

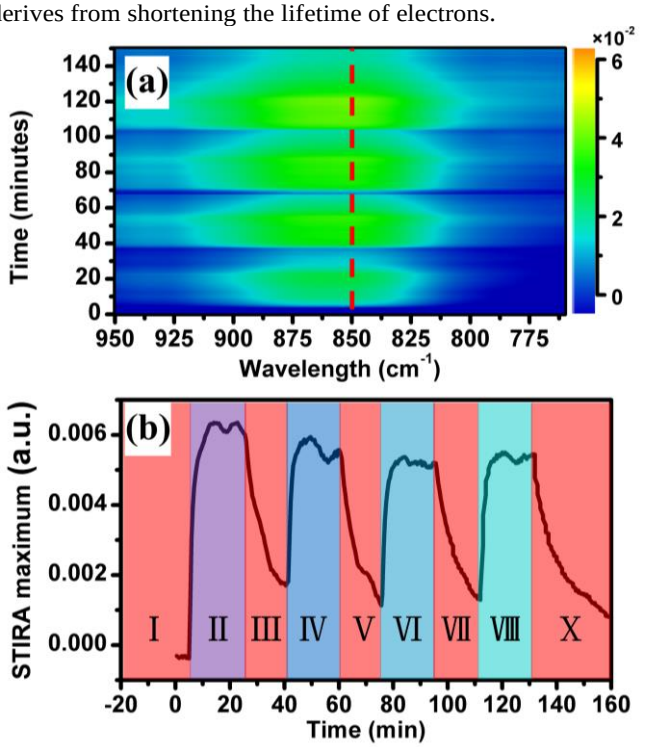

Figure 6. (a) In-situ ATR-IR spectra of Au/TiO_2 during green and UV light irradiation with different power. (b) Plot of the temporal variation of absorbance of the peak at ~850 cm^{-1}. The processes of Ⅰ, Ⅲ, Ⅴ, Ⅶ and Ⅹ were in the dark. the power ratios of green to UV light of Ⅱ, Ⅳ, Ⅵ and Ⅷ were 0W/1W, 0.3W/1W, 0.5W/1W, 1W/1W, respectively. All of back-ground spectrums are before the light irradiation.

However, there must exist some mechanisms of LSPR enhances the photocatalytic activity of Au/TiO_2 under UV-Vis light irradiation. Jen and coworkers have proved that near field intensity enhancement of LSPR effectively increases the photocatalytic process.[56] Certainly, it is one of important mechanisms for the activity enhancement. But here, we proposed that many hot electrons exist at the Au NPs surfaces due to LSPR is the key.[6, 29] In other words, LSPR acts to donate hot electrons into available adsorbate states on the surfaces of Au NPs is the key to its positive effect. Because of joining the collective oscillation, the electrons which are close to the interface have more opportunities to move to the Au NPs surfaces, then decay and become the hot electrons captured by acceptors.[46] In order to disclose the behavior of collective oscillation, Finite Element Method (FEM) was performed to calculate the charge distribution driven by incident light in gold nanoparticle (Au NP) (as shown in Figure 7, see Supporting Information for details). During the simulation, the diameters of the Au NP and TiO_2 were 10 nm and 50 nm, respectively, and the wavelength of incident light is 575 nm. When the Au/TiO_2 is illuminated by light with the wavelength much larger than the size of Au NP, the charge density of Au NP is redistributed.[57] Then a coulombic restoring force appeared and the charge density coherently oscillates in phase with the incident light.[2]

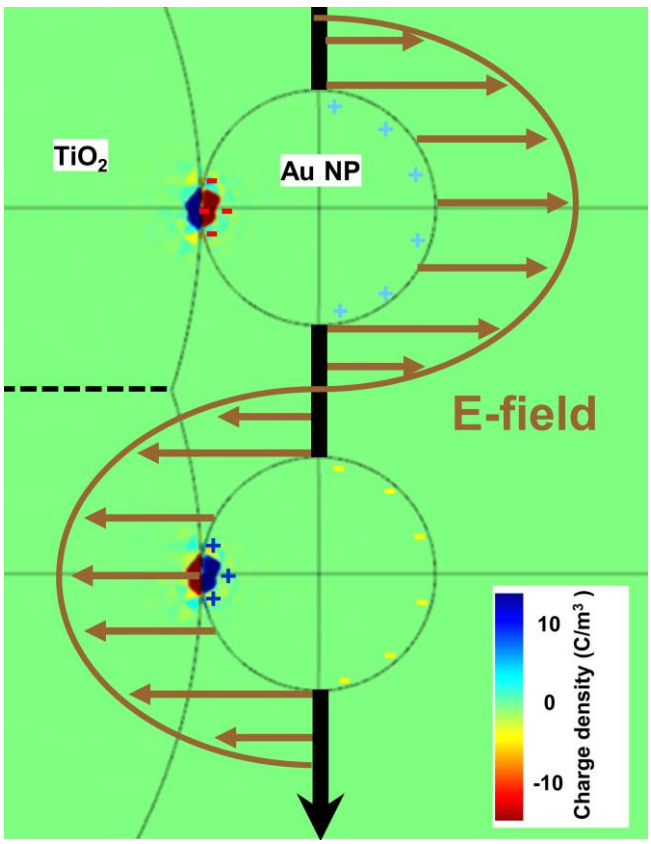

Figure 7. The changes of charge density of Au NP were induced by the electric field component of incident light. The wavelength of incident light is 575 nm.

According to above analysis, the whole mechanism for LSPR affects the photocatalytic activity of Au/TiO_2 under UV-Vis light irradiation can be depicted in Scheme 1. Firstly, the electron and hole pairs are produced by UV radiation in TiO_2, and some of the electrons (shallow trapped electrons) can be trapped and tend to reduce Ti^{4+} cations to Ti^{3+} states,[58] some of the electrons (Au trapped electrons) surmount the SB and localized in adjacent Au NPs. Then, on the one hand, the Au trapped electrons driven by LSPR in response to the incident green light, have more opportunities to reach the Au NPs surfaces, thus the acceptors capture them becomes easier. This is the positive side of LSPR affects the photocatalytic performance of Au/TiO_2. One the other hand, the Au NPs can inject the Au trapped electrons back into the TiO_2 due to LSPR, hence the time of electrons reside in the Au NPs is shortened in comparison with merely under the irradiation of UV light. This process will promote the recombination of electrons and holes to a certain extent, and impairs the photocatalysis. In conclusion, when employing with UV-Vis mixing light irradiation, both pros and cons exist simultaneously for the LSPR brings to photocatalytic reaction of Au/TiO_2. When it comes to the question that which mechanism and to what extent would the above two competitors dominate the overall photocatalytic reaction, it depends on the intensity ratio of visible to UV light employed to the Au/TiO_2 structure. In the combination with above results of photocatalytic experiment, the variations of two sides with the intensity ratio of visible to UV light are discussed as follows.

The photocatalytic activity of 0.8/10W/Au/TiO_2 exhibits high efficiency, which indicates that the positive effect can show strong response as soon as LSPR take place in Au NPs. While the negative effect is not obvious, because the change of photogenerated electrons lifetime is very small at this situation in despite of its rate of change is exceedingly fast. As the intensity of LSPR continues to rise, photocatalytic activity starts to decline, such as 2.2/10W/Au/TiO_2 and 4.5/10W/Au/TiO_2, hints that when the intensity of LSPR is not so high, the increase of positive effect is slower than the negative effect. But after 9/10W/Au/TiO_2, the photocatalytic activity increase again, suggests that the incremental rate of positive effect begin to catch up with negative effect. The relationships between the effects of two sides and the intensity ratios of visible to UV light can be described qualitatively in Figure 8.

Scheme 1. The whole mechanism for LSPR affects the photocatalytic activity of Au/TiO_2 under UV-Vis light irradiation.

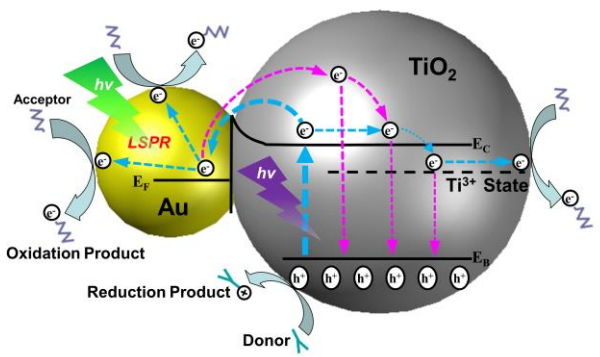

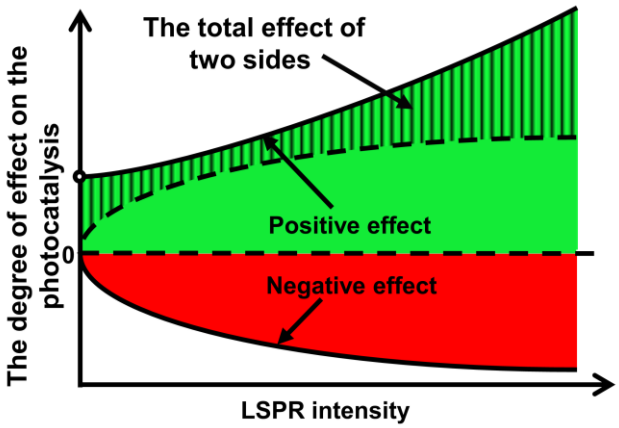

Figure 8. Qualitative variations of positive (green area) and negative (red area) caused by increasing intensity ratio of visible to UV light. Shaded part represents the general effects of two sides.

Conclusions

The photocatalytic activities of Au/TiO_2 towards MB reaction under different power ratios of green to UV light irradiation have been investigated. Specially, it has been shown that, with increasing power ratio, the photocatalytic activity increased initially and then decreased, but increased again at last. For this case, we have proposed that it results from the coexistence of positive and negative effects of LSPR on the photocatalysis. Through the *I–V* characteristics of Au/TiO_2 measured by CAFM, we have demonstrated the formation of SB between Au NPs and TiO_2. Then, the STIRA of green light irradiated Au/TiO_2 demonstrated the hot electrons generated from LSPR decay in Au NPs, which had sufficient energy to overleap the SB and flow into the TiO_2. Asides from the positive effect of LSPR that the hot electrons existing on the Au NPs surfaces would favor the photocatalytic reaction, we have proved that when operating under mixing UV and green light irradiation, the LSPR injected hot electrons (from Au NPs to TiO_2) may compensate those transferred from TiO_2 to Au NPs, thus shorten the lifetime of UV excited electrons in TiO_2 and hence may impair the overall photocatalyic performance. This provided us with a more profound understanding of photocatalysis mechanism under UV-Vis light irradiation, along with an instructive direction for the next generation composite photocatalyst design.

Acknowledgements

This research was supported by Shanghai Science and Technology Committee (10PJ1403800, 11DZ1111200), Yunnan Provincial Science and Technology Department (2010AD003), National Natural Science Foundation of China (21103104, 61204129). The authors would also like to acknowledge the Instrumental Analysis & Research Center of Shanghai University for XRD, XPS characterization assistance.

Notes and references

[a] Department of Physics, College of Science, Shanghai University, Shanghai, 200444, China

[b] Department of Chemistry, College of Science, Shanghai University, Shanghai 200444, China

[c] Institute of NanoMicroEnergy, Shanghai University, Shanghai 200444, China. Fax/ Tel: +81-21-66135201; E-mail: zhiyuhu@sjtu.edu.cn

[d] School of Materials Science and Engineering, Shanghai University, Shanghai 200072, China

[e] National Key Laboratory of Science and Technology on Micro/Nano Fabrication, Department of Micro/Nano Electronics, Shanghai Jiao Tong University, Shanghai 200240, China

† Electronic Supplementary Information (ESI) available: Detailed description of the calculation parameters. Additional I-V characteristics of bare TiO_2 and the tip of CAFM probe. See DOI: 10.1039/b000000x/

1. M. Miljevic, B. Geiseler, T. Bergfeldt, P. Bockstaller and L. Fruk, *Adv Funct Mater*, 2014, **24**, 907-915.
2. X. Zhou, G. Liu, J. Yu and W. Fan, *J. Mater. Chem*, 2012, **22**, 21337.
3. Z. W. Seh, S. Liu, M. Low, S.-Y. Zhang, Z. Liu, A. Mlayah and M.-Y. Han, *Advanced materials*, 2012, **24**, 2310-2314.
4. I. Dolamic and T. Bürgi, *J. Phys. Chem. C* 2011, **115**, 2228-2234.
5. Á. Veres, T. Rica, L. Janovák, M. Dömök, N. Buzás, V. Zöllmer, T. Seemann, A. Richardt and I. Dékány, *Catal Today*, 2012, **181**, 156-162.
6. S. Linic, P. Christopher and D. B. Ingram, *Nature materials*, 2011, **10**, 911-921.
7. Y. Nosaka, M. Matsushita, J. Nishino and A. Y. Nosaka, *Sci Technol Adv Mat*, 2005, **6**, 143-148.
8. Q. Xiang and J. Yu, *J. Phys. Chem. Lett*, 2013, **4**, 753-759.
9. A. A. Ismail and D. W. Bahnemann, *J. Phys. Chem. C* 2011, **115**, 5784-5791.
10. M. M. M. C. Hidalgo, Jose´ A. Navı´o, and Gerardo Colo´n, *J. Phys. Chem. C*, 2009, **113**, 12840–12847.
11. J. Yan, G. Wu, N. Guan and L. Li, *Chem Commun*, 2013, **49**, 11767-11769.
12. A. Polman, *Science*, 2008, **322**, 868-869.
13. E. Kowalska, R. Abe and B. Ohtani, *Chem Commun*, 2009, 241-243.
14. V. Iliev, D. Tomova, L. Bilyarska and G. Tyuliev, *J. Mol. Catal. A-Chem*, 2007, **263**, 32-38.
15. X. Zhang, Y. L. Chen, R. S. Liu and D. P. Tsai, *Reports on progress in physics. Physical Society*, 2013, **76**, 046401.
16. R. Kraya, L. Y. Kraya and D. A. Bonnell, *Nano letters*, 2010, **10**, 1224–1228.
17. T. Yang, S. Hertenberger, S. Morkötter, G. Abstreiter and G. Koblmüller, *Appl Phys Lett*, 2012, **101**, 233102.
18. R.A.Kraya and L.Y.Kraya, *J.Appl.Phys*, 2012, **111**, 064302-064301-064304.
19. T. Berger, M. Sterrer, O. Diwald, E. Knözinger, D. Panayotov, T. L. Thompson, J. T. Yates and Jr, *J. Phys. Chem. B*, 2005, **109**, 6061-6068.
20. D. M. Savory, D. S. Warren and A. J. McQuillan, *J. Phys. Chem. C*, 2011, **115**, 902.
21. D. M. Savory and A. J. McQuillan, *J. Phys. Chem. C*, 2013, **117**, 23645-23656.
22. X. Shi, K. Ueno, T. Oshikiri and H. Misawa, *J. Phys. Chem. C* 2013, **117**, 24733-24739.
23. Y. H. Jang, Y. J. Jang, S. T. Kochuveedu, M. Byun, Z. Lin and D. H. Kim, *Nanoscale*, 2014, **6**, 1823-1832.
24. C. Nahm, H. Choi, J. Kim, D.-R. Jung, C. Kim, J. Moon, B. Lee and B. Park, *Appl Phys Lett*, 2011, **99**, 253107.
25. M. Alvaro, B. Cojocaru, A. A. Ismail, N. Petrea, B. Ferrer, F. A. Harraz, V. I. Parvulescu and H. Garcia, *Appl Cataly B-Environ*, 2010, **99**, 191-197.
26. M. A. Centeno, M. C. Hidalgo, M. I. Dominguez, J. A. Navío and J. A. Odriozola, *Catal Lett*, 2008, **123**, 198-206.
27. A. Zwijnenburg, A. Goossens, W. G. Sloof, M. W. J. Craje, A. M. v. d. Kraan, L. J. d. Jongh, M. Makkee and J. A. Moulijn, *J. Phys. Chem. B* 2002, **106**, 9853-9862.
28. W. Haiss, N. T. K. Thanh, J. Aveyard and D. G. Fernig, *Anal.Chem*, 2007, **79**, 4215-4221.
29. S. Mukherjee, F. Libisch, N. Large, O. Neumann, L. V. Brown, J. Cheng, J. B. Lassiter, E. A. Carter, P. Nordlander and N. J. Halas, *Nano letters*, 2013, **13**, 240-247.
30. S.-Y. Du and Z.-Y. Li, *Optics letters*, 2010, **35**, 3402-3404.
31. J. Butet, I. Russier-Antoine, C. Jonin, N. Lascoux, E. Benichou and P.-F. Brevet, *The Journal of Physical Chemistry C*, 2013, **117**, 1172-1177.
32. J. Y. Park, J. R. Renzas, B. B. Hsu and G. A. Somorjai, *J. Phys. Chem. C* 2007, **111**, 15331-15336.
33. C. Yogi, K. Kojima, T. Hashishin, N. Wada, Y. Inada, E. Della Gaspera, M. Bersani, A. Martucci, L. Liu and T.-K. Sham, *J. Phys. Chem. C* 2011, **115**, 6554-6560.
34. X.-H. Li, M. Baar, S. Blechert and M. Antonietti, *Sci Rep-Uk*, 2013, **3**, 1743.
35. P. Wang, B. Huang, Y. Dai and M. H. Whangbo, *Physical chemistry chemical physics : PCCP*, 2012, **14**, 9813-9825.
36. P. A. DeSario, J. J. Pietron, D. E. DeVantier, T. H. Brintlinger, R. M. Stroud and D. R. Rolison, *Nanoscale*, 2013, **5**, 8073-8083.
37. E. E. W. Vaidyanathan Subramanian, and Prashant V. Kamat, *J. Am. Chen. Soc*, 2004, **126**, 4943 -4950.
38. S. S. Naik and V. R. Reddy, *Superlattice Microst*, 2010, **48**, 330-342.
39. N. Spyropoulos-Antonakakis, E. Sarantopoulou, Z. Kollia, Z. Samardžija, S. Kobe and A. C. Cefalas, *J.Appl.Phys*, 2012, **112**, 094301.
40. A. O. Govorov, H. Zhang and Y. K. Gun'ko, *J. Phys. Chem. C* 2013, **117**, 16616-16631.
41. H. Yoo, C. Bae, Y. Yang, S. Lee, M. Kim, H. Kim, Y. Kim and H. Shin, *Nano letters*, 2014, **14**, 4413-4417.
42. E. Dupont-Ferrier, P. Mallet, L. Magaud and J. Y. Veuillen, *Phys Rev B*, 2007, **75**.
43. L. Yang, C. Kuegeler, K. Szot, A. Ruediger and R. Waser, *Appl Phys Lett*, 2009, **95**, 013109.
44. D. S. Warren and A. J. McQuillan, *J. Phys. Chem. B*, 2004, **108**, 19373-19379.
45. L.-B. Xiong, J.-L. Li, B. Yang and Y. Yu, *J. Nanomater*, 2012, **2012**, 1-13.
46. S. Mukherjee, L. Zhou, A. M. Goodman, N. Large, C. Ayala-Orozco, Y. Zhang, P. Nordlander and N. J. Halas, *J. Am. Chen. Soc*, 2014, **136**, 64-67.
47. A. Furube, L. Du, K. Hara, R. Katoh and M. Tachiya, *J. Am. Chem. Soc*, 2007,, , 14852-14853.
48. Z. Bian, T. Tachikawa, P. Zhang, M. Fujitsuka and T. Majima, *J. Am. Chen. Soc*, 2014, **136**, 458-465.
49. A. Yamakata, T.-a. Ishibashi and H. Onishi, *J Photoch Photobio A*, 2003, 33-36.
50. A. Yamakata, T.-a. Ishibashi and H. Onishi, *J. Mol. Catal. A-Chem*, 2003, 85-94.
51. T. L.Thompson, J. T. Yates and Jr, *Chem Rev*, 2006, **106**, 4428-4453.
52. L. Jing, J. Zhou, J. R. Durrant, J. Tang, D. Liu and H. Fu, *Energ Environ. Sci*, 2012, **5**, 6552–6558.
53. K. Pomoni, A. Vomvas and C. Trapalis, *Thin Solid Films*, 2005, 160-165.
54. Z. Zhang and J. John T. Yates, *J. Phys. Chem. B*, 2010, **114**, 3098-3101.
55. L. Braginsky and V. Shklover, *Eur. Phys. J. D*, 1999, 627-630.
56. J.-J. Chen, J. C. S. Wu, P. C. Wu and D. P. Tsai, *J. Phys. Chem. C* 2012, **116**, 26535-26542.
57. J. Aizpurua, G. W. Bryant, L. J. Richter and F. J. G. d. Abajo, *PHYSICAL REVIEW B*, 2005, **71**, 235420.
58. A. I. Kuznetsov, O. Kameneva, A. Alexandrov, N. Bityurin, K. Chhor and A. Kanaev, *J. Phys. Chem. B*, 2006, **110**, 435-441.

A graphic entry for the Table of Contents (TOC)